Research Square

Preprints are preliminary reports that have not undergone peer review.
They should not be considered conclusive, used to inform clinical practice,
or referenced by the media as validated information.

Chronic Circadian Desynchrony Disrupts Stage-Specific Spermiogenesis and Male Fertility

Alisa P Becin
University of Novi Sad, Faculty of Sciences
Dusan Lalosevic
University of Novi Sad, Medical Faculty
Silvana A Andric
University of Novi Sad, Faculty of Sciences
Tatjana S Kostic
tatjana.kostic@dbe.uns.ac.rs

University of Novi Sad, Faculty of Sciences

Article

Keywords: Spermatids, Spermatozoa, Circadian disturbance, Clock, Mitochondria

Posted Date: August 27th, 2026

DOI: https://doi.org/10.21203/rs.3.rs-10625211/v1

License: This work is licensed under a Creative Commons Attribution 4.0 International License.
Read Full License

Additional Declarations: No competing interests reported.

Abstract

Circadian disruption is increasingly associated with male reproductive dysfunction, yet the developmental stages underlying this relationship remain poorly defined. We investigated whether chronic circadian desynchrony disrupts the stage-specific molecular and bioenergetic organization of spermiogenesis and compromises male fertility. Adult Wistar rats were maintained under a standard light-dark cycle or exposed for two months to repeated cycles of constant light, constant darkness, and light-dark conditions. Round spermatids, elongated spermatids, and epididymal spermatozoa were analyzed for clock and mitochondria-related gene expression and mitochondrial bioenergetics. Under control conditions, spermiogenesis exhibited coordinated stage- and time-dependent transcriptional and bioenergetic organization, with developing spermatids relying predominantly on oxidative phosphorylation. Circadian desynchrony reduced circulating testosterone and the abundance of elongated spermatids and disturbed stage-specific clock and mitochondrial gene expression, with the most pronounced transcriptional alterations in elongated spermatids. Bioenergetic responses were also stage dependent: ATP production increased in round spermatids but decreased in elongated spermatids and spermatozoa, accompanied by altered mitochondrial homeostasis. Circadian desynchrony also impaired progesterone-induced acrosome reaction and reduced reproductive success. These findings identify spermiogenesis as a circadian-sensitive developmental process and highlight elongated spermatids as a particularly vulnerable stage linking disrupted temporal organization and mitochondrial dysfunction to impaired male fertility.

Introduction

Infertility affects approximately 8–12% of couples worldwide, with male factors contributing to nearly half of all cases (1, 2). Despite substantial advances in the diagnosis of male reproductive disorders, a large proportion of men remain classified as having idiopathic infertility, indicating that the molecular mechanisms governing male reproductive competence are still incompletely understood. Increasing evidence suggests that environmental and lifestyle factors, particularly circadian disruption, contribute to impaired male reproductive function (3, 4, 5).

Male reproductive physiology exhibits circadian organization, whereby rhythmic endocrine secretion is synchronized with the responsiveness of target tissues (6). Daily oscillations in testosterone secretion and several parameters of sperm production and semen quality indicate that successful spermatogenesis depends on precise temporal coordination between endocrine signaling and germ-cell developmental programs (7, 8, 9, 10). Among the stages of germ-cell development, spermiogenesis is characterized by extensive structural and metabolic remodeling, including chromatin condensation, acrosome formation, mitochondrial reorganization, and flagellar development (11, 12, 13). These developmental events impose high energetic demands that require coordinated regulation of mitochondrial biogenesis, oxidative metabolism, mitochondrial dynamics, and quality-control mechanisms (14, 15, 16, 17).

Recent studies have advanced our understanding of circadian regulation within the testis by demonstrating extensive rhythmic gene expression and identifying the Sertoli-cell circadian clock as a regulator of retinoic acid signaling required for spermatogonial differentiation and male fertility (18). These findings established germ-cell development as a target of peripheral circadian regulation and challenged the long-standing view that the testis lacks functional circadian organization (19). However, whether circadian regulation also coordinates the stage-specific molecular and metabolic remodeling that characterizes spermiogenesis remains unknown.

In metabolically active tissues, the molecular circadian clock is closely integrated with mitochondrial homeostasis through regulation of mitochondrial biogenesis, oxidative metabolism, mitochondrial dynamics, and mitophagy (14, 15, 16, 20). Disruption of this regulatory network impairs mitochondrial function and cellular metabolism. Although mitochondria are essential for germ-cell differentiation and sperm function, whether circadian mechanisms regulate mitochondrial homeostasis during spermiogenesis has not been established.

Our previous studies demonstrated that chronic circadian desynchrony impairs testicular endocrine function and sperm quality (21, 22), suggesting that developing germ cells are particularly susceptible to circadian disruption. However, the stage-specific molecular events linking circadian desynchrony with impaired sperm function remain undefined.

Therefore, the present study investigated whether chronic circadian desynchrony disrupts the stage-specific molecular organization of spermiogenesis by altering circadian clock signaling and mitochondrial homeostasis. Using isolated round spermatids, elongated spermatids, and epididymal spermatozoa, we examined the expression of circadian clock genes together with genes regulating mitochondrial biogenesis, oxidative metabolism, mitochondrial dynamics, and mitophagy, and evaluated mitochondrial bioenergetics, sperm functional competence, and reproductive outcome. We hypothesized that chronic circadian desynchrony disrupts the coordinated molecular and bioenergetic organization required for normal spermiogenesis, thereby compromising sperm function and male fertility.

Results

Circadian desynchrony alters endocrine rhythmicity and selectively impairs early spermatid maturation. Adult rats were exposed to an altered light schedule for two months and evaluated at two circadian time points corresponding to the inactive (ZT11) and active (ZT23) phases. Successful induction of circadian desynchrony was confirmed by continuous locomotor activity monitoring, which revealed reduced voluntary activity and disruption of the normal daily activity pattern (Fig. 1A). Because spermiogenesis depends on endocrine regulation, blood testosterone levels were analyzed. Under LD conditions, testosterone exhibited a clear diurnal rhythm, with higher concentrations at ZT11 than at ZT23 (Fig. 1B). Circadian desynchrony reduced testosterone concentrations at both time points and markedly increased interindividual variability during the active phase (ZT23; LD: 32.0% vs CD: 112.0%), indicating impaired endocrine rhythmicity and hormonal stability.

To determine whether endocrine disruption affected spermatid differentiation, ES were quantified at stage VII of the seminiferous epithelium, one of the most androgen-dependent and metabolically demanding stages of spermiogenesis (26). CD significantly reduced the abundance of ES (Fig. 1C), indicating impaired progression through late spermatid differentiation.

To further define the developmental stage affected by circadian desynchrony, we analyzed the expression of the spermatid differentiation markers *Tnp1* and *Prm2* (27) in isolated RS and ES. As expected, *Tnp1* was predominantly expressed in RS, whereas *Prm2* was enriched in ES, confirming successful germ-cell separation (Fig. 1D, E). Under LD conditions, *Tnp1* exhibited marked time-of-day variation, peaking at ZT11 in RS and ZT23 in ES, whereas *Prm2* expression remained relatively stable in RS and increased during spermatid elongation (Fig. 1D, E).

CD selectively reduced *Tnp1* expression in both RS and ES (Fig. 1D), whereas *Prm2* expression remained largely unchanged, except for a reduction at ZT23 in ES (Fig. 1E). Together with the histologically confirmed reduction in ES abundance (Fig. 1C), these findings indicate that CD primarily impairs the early transcriptional events preceding chromatin condensation.

Obtained data demonstrate that CD disrupts endocrine rhythmicity and selectively compromises early spermatid differentiation. This prompted us to investigate whether normal spermiogenesis is characterized by stage-specific temporal organization of circadian clock and mitochondria-related gene expression, and whether this developmental program is disrupted by circadian desynchrony.

Stage-specific circadian programming is accompanied by coordinated mitochondrial organization during spermiogenesis

To characterize the physiological temporal organization of spermiogenesis, RS, ES, and epididymal Sp were isolated from LD animals at ZT11 and ZT23, and the expression of circadian clock genes together with genes regulating mitochondrial biogenesis, dynamics, quality control, and oxidative metabolism was analyzed.

Principal component analysis (PCA) revealed a clear stage-specific organization of clock gene expression during spermiogenesis (Fig. 2A). The first two principal components explained 77.9% of the total variance, separating spermatozoa from developing spermatids, with elongated spermatids occupying an intermediate position between round spermatids and spermatozoa. Genes comprising the negative arm of the molecular clock (*Per1*, *Per2*, *Cry1*, *Cry2*, and *Reverbb*) were primarily associated with spermatozoa, whereas *Bmal1*, *Reverba*, and *Rora* were associated with spermatids, indicating stage-specific reorganization of the molecular circadian program during germ-cell differentiation.

Consistent with the PCA, quantitative analysis showed that most clock genes progressively declined during spermiogenesis (Fig. 2C). Although transcript abundance was markedly lower in spermatozoa

than in spermatids for most genes, *Rora* remained relatively abundant in mature spermatozoa. Most clock genes also exhibited coordinated time-of-day variation, with higher expression at ZT11 than ZT23, whereas *Rora* displayed a distinct stage-specific expression pattern.

A similar stage-specific organization was observed for mitochondria-related genes. PCA explained 81.7% of the total variance and clearly separated RS, ES, and Sp into distinct transcriptional clusters (Fig. 2B). Mitochondria-related genes exhibited even greater stage-dependent segregation than clock genes, indicating extensive transcriptional reorganization of mitochondrial pathways during spermiogenesis. While genes regulating mitochondrial biogenesis, oxidative phosphorylation, and dynamics clustered together, *Tfam* and *Tfeb* showed distinct loading patterns, suggesting stage-specific regulation during germ-cell differentiation.

Heatmap analysis further demonstrated extensive stage-specific and time-of-day-dependent organization of mitochondria-related gene expression (Fig. 2D). Round spermatids exhibited the highest expression of genes involved in mitochondrial biogenesis (*Ppargc1a*, *Tfam*, and *Nrf1*), oxidative metabolism (*Cytc* and *Cox4i2*), mitochondrial fusion (*Mfn1*, *Mfn2*, and *Opa1*), fission (*Drp1* and *Fis1*), and mitophagy (*Pink1* and *Prkn*), with consistently higher expression at ZT11 than at ZT23. This coordinated transcriptional program progressively declined during differentiation, although low-abundance transcripts of mitochondrial biogenesis-related genes (*Ppargc1a*, *Nrf1*, *Tfam*, *Cytc*, and *Cox4i2*) remained detectable in spermatozoa, suggesting that most mitochondrial remodeling is completed before the end of spermiogenesis.

To determine whether these transcriptional changes were accompanied by alterations in cellular bioenergetics, ATP production was analyzed in the presence and absence of oligomycin (Fig. 2E,F). Under basal conditions, ATP content was highest in spermatozoa compared with round and elongated spermatids. Oligomycin markedly reduced ATP levels in both spermatid populations, indicating that ATP production during spermatid differentiation depends predominantly on mitochondrial oxidative phosphorylation. In contrast, spermatozoa retained a substantial proportion of ATP following oligomycin treatment, demonstrating a reduced dependence on mitochondrial respiration (Fig. 2E, F).

Quantification of oligomycin-sensitive ATP production confirmed a stage-specific bioenergetic transition during spermiogenesis (Fig. 2F). Whereas developing spermatids derived most of their ATP from mitochondrial oxidative phosphorylation, spermatozoa relied substantially more on glycolysis. Together, these findings establish coordinated stage-specific organization of circadian clock gene expression, mitochondria-related gene expression, and cellular bioenergetics during normal spermiogenesis. The effects of circadian desynchrony on this developmental program were subsequently evaluated.

Chronic circadian desynchrony disrupts stage-specific mitochondrial homeostasis during spermiogenesis

Clock genes together with genes regulating mitochondrial biogenesis, oxidative metabolism, mitochondrial dynamics, and quality control were analyzed in RS, ES, and Sp from LD and CD animals collected at ZT11 and ZT23 (Fig. 3). Under LD conditions, clock genes exhibited coordinated stage- and time-dependent expression throughout spermiogenesis. CD disrupted this temporal organization across all germ-cell populations, primarily by attenuating normal time-of-day differences rather than inducing uniform changes in transcript abundance. Alterations involved several core clock genes, including *Bmal1*, *Clock*, *Per1*, *Per2*, *Reverba*, and *Reverbb*, with the greatest disruption observed in ES and Sp, particularly at ZT23, whereas RS remained comparatively preserved.

A similar pattern was observed for mitochondria-related genes. Under control conditions, genes regulating mitochondrial biogenesis (*Ppargc1a*, *Tfam*, *Nrf1*), oxidative metabolism (*Cytc*, *Cox4i2*), mitochondrial dynamics (*Mfn1*, *Mfn2*, *Opa1*, *Drp1*, and *Fis1*), and mitophagy (*Pink1* and *Prkn*) exhibited coordinated stage- and time-dependent expression during spermiogenesis (Fig. 2D). CD disrupted this developmental organization across all germ-cell populations, predominantly by attenuating normal time-of-day differences, with the greatest alterations observed in ES and Sp, particularly at ZT23 (Fig. 3).

Overall, CD disrupted the coordinated stage- and time-dependent organization of clock- and mitochondria-related gene expression during spermiogenesis, with ES showing the greatest transcriptional alterations. We next examined whether these molecular changes were accompanied by alterations in mitochondrial bioenergetics and integrity.

ATP measurements revealed distinct stage-dependent effects of CD (Fig. 3B). Compared with LD, ATP content increased in RS but decreased markedly in ES and Sp. Oligomycin markedly reduced ATP levels in both LD and circadian-desynchronized RS and ES, confirming their predominant dependence on oxidative phosphorylation. In contrast, oligomycin produced little additional reduction in ATP levels in Sp following circadian desynchrony, indicating that mitochondrial ATP production was already compromised under these conditions (Fig. 3B).

To determine whether these bioenergetic changes were associated with altered mitochondrial homeostasis, mitochondrial membrane potential (Δψm, assessed by TMRE fluorescence), mitochondrial content (MitoTracker), and mitochondrial DNA abundance (determined as the *Mt-Nd1*/*B2m* ratio) were assessed (Fig. 3C-E). Circadian desynchrony increased Δψm in ES, whereas RS remained unaffected and no significant change was observed in Sp (Fig. 3C). Mitochondrial content and mtDNA copy number were increased in both RS and ES but remained unchanged in Sp (Fig. 3D,E).

Together, these findings indicate that CD disrupts mitochondrial homeostasis in a stage-dependent manner, with ES exhibiting the most pronounced impairment of mitochondrial bioenergetics and integrity.

Circadian desynchrony compromises sperm functional competence and reduces male reproductive success

The ability of capacitated spermatozoa to undergo progesterone-induced acrosome reaction was evaluated as a functional indicator of fertilizing competence (Fig. 4A). Under LD conditions, progesterone stimulation induced the expected increase in the proportion of acrosome-reacted Sp. In contrast, Sp obtained from circadian-desynchronized animals exhibited a significantly reduced acrosome response at both ZT11 and ZT23 (Fig. 4B, C), indicating diminished responsiveness to physiological stimulation.

To determine whether these functional impairments were reflected in reproductive outcome, circadian-desynchronized males were mated with control females. Males exposed to circadian desynchrony produced fewer offspring than control males (Fig. 4D). In addition, the number of offspring per mate was lower and exhibited greater interindividual variability in the circadian-desynchronized group (Fig. 5E), indicating reduced reproductive performance.

Overall, these findings demonstrate that the effects of CD extend from spermatid differentiation and mitochondrial homeostasis to sperm function and reproductive success.

Discussion

The present study demonstrates that spermiogenesis is a circadian-sensitive developmental process characterized by coordinated stage-specific organization of circadian signaling, mitochondrial homeostasis, and cellular bioenergetics. Chronic circadian desynchrony disrupted this developmental program, resulting in endocrine instability, mitochondrial dysfunction, impaired sperm function, and reduced reproductive success, identifying spermiogenesis as a target of circadian regulation (Supplemental Material – Graphical Abstract).

Previous experimental studies, including our own, have shown that chronic circadian disruption impairs testicular endocrine function and sperm quality (21, 22, 10). While Leydig cells are recognized as the principal circadian oscillator in the testis (7, 28), recent findings indicate that circadian regulation is not restricted to steroidogenic cells. Liu et al. demonstrated that the molecular clock in Sertoli cells regulates retinoic acid biosynthesis, thereby synchronizing spermatogonial differentiation and reinforcing the concept of the testis as a circadian-responsive organ (18). Our previous work demonstrated coordinated expression of core-clock and mitochondria-related genes in epididymal spermatozoa following chronic circadian desynchrony (22). Here, we show that temporal organization associated with the circadian system extends to the later stages of spermatogenesis. Although only two circadian time points were analyzed, disruption of the stage-specific organization of clock and mitochondria-related genes indicates loss of temporal coordination during germ-cell maturation.

The transition from RS to ES emerged as the developmental stage most susceptible to circadian disruption. This transition largely corresponds to stage VII of the seminiferous epithelium, one of the most androgen-dependent and metabolically demanding phases of spermatogenesis (26). During this developmental window, chromatin condensation, acrosome formation, flagellar assembly, mitochondrial redistribution, and cytoplasmic remodeling occur simultaneously, imposing substantial energetic

demands on developing germ cells (29). Successful completion of this transition requires precise temporal coordination of the transcriptional program governing chromatin remodeling, including the sequential expression of *Tnp1* and *Prm2*, which mediate histone replacement and protamine-dependent chromatin condensation (30, 31, 27). Disruption of these genes has been associated with defective chromatin packaging, abnormal sperm morphology, reduced motility, impaired fertilizing capacity, and male infertility (32, 33). Our previous study demonstrated that chronic circadian desynchrony alters the temporal expression of *Tnp1* and *Prm2* in whole seminiferous tubules (22). The present study demonstrates that circadian desynchrony disrupts the expression of both genes within isolated RS and ES, with *Tnp1* being particularly affected, indicating that the molecular events preceding chromatin condensation are especially sensitive to circadian disruption. These molecular alterations were accompanied by reduced blood testosterone, increased endocrine variability, and a decreased abundance of ES at stage VII. Together, these findings suggest that successful spermiogenesis depends not only on adequate androgen availability but also on precise temporal coordination between endocrine signaling and stage-specific germ-cell developmental programs. Given the established role of testosterone in regulating both spermatid differentiation and mitochondrial homeostasis (34, 35), disruption of this temporal coordination may represent an important upstream mechanism linking circadian desynchrony to the mitochondrial dysfunction observed during germ-cell maturation.

Spermiogenesis is accompanied by a coordinated developmental transition in mitochondrial energy metabolism (36, 37). Consistent with this concept, RS and ES relied predominantly on oxidative phosphorylation, whereas Sp became less dependent on mitochondrial ATP production. Chronic circadian desynchrony disrupted this bioenergetic transition in a stage-specific manner. RS exhibited increased ATP production together with higher mitochondrial content, consistent with an adaptive response aimed at preserving mitochondrial homeostasis during the early phases of spermiogenesis. In contrast, ES displayed reduced ATP production despite increased mitochondrial membrane potential, mitochondrial content, suggesting that these adaptive mitochondrial responses are insufficient to maintain bioenergetic function as differentiation progresses. Consequently, the transition from RS to ES appears to represent a critical developmental window during which disruption of temporal coordination has the greatest impact on mitochondrial homeostasis. These mitochondrial alterations persisted in Sp, which exhibited reduced ATP production together with loss of oligomycin sensitivity, indicating impaired mitochondrial bioenergetic function.

Although direct mechanistic relationships were not examined in the present study, substantial experimental evidence supports functional interactions between the molecular circadian clock and mitochondrial homeostasis. BMAL1 and REVERBA regulate mitochondrial biogenesis through the SIRT1–PGC-1α signaling axis, thereby controlling the expression of NRF1, TFAM, CYTC, and other key regulators of oxidative metabolism (38, 39, 40). Circadian control also extends to mitochondrial dynamics: rhythmic DRP1 phosphorylation has been shown to coordinate mitochondrial fission with circadian oscillations in ATP production (41), whereas CLOCK regulates *Drp1* mRNA stability (42). These mechanisms provide a plausible biological framework linking disruption of clock gene expression with altered mitochondrial dynamics and bioenergetics observed during spermiogenesis.

The progressive reduction of transcript abundance observed during germ-cell maturation is consistent with the extensive chromatin condensation and transcriptional silencing accompanying spermiogenesis (43, 44). The residual clock- and mitochondria-related transcripts detected in spermatozoa most likely represent a molecular memory of spermatogenesis rather than ongoing transcription, consistent with the extensive chromatin condensation accompanying sperm maturation (43, 45). Alterations in sperm RNA composition following circadian desynchrony may therefore serve as biomarkers of disrupted spermatogenesis while potentially influencing early embryonic development.

The biological significance of these molecular and mitochondrial alterations was demonstrated by impaired sperm function and reduced reproductive performance. Circadian desynchrony significantly reduced progesterone-induced acrosome reaction, indicating compromised functional competence of spermatozoa, and was accompanied by decreased reproductive success in mating experiments. These observations demonstrate that disruption of mitochondrial remodeling during spermiogenesis translates into measurable impairment of fertilization capacity and male fertility (46, 47, 48). From a clinical perspective, these findings provide support for epidemiological studies reporting reduced fertility among men exposed to chronic circadian disruption, including shift workers and individuals experiencing prolonged circadian misalignment (3, 35, 49, 50, 5).

Several limitations should be acknowledged. Because gene expression was assessed at only two circadian time points, the findings should be interpreted as evidence of disrupted temporal coordination rather than altered circadian rhythmicity. In addition, the molecular mechanisms linking clock disruption with mitochondrial dysfunction were not directly investigated and warrant further study.

In conclusion, the present study demonstrates that spermiogenesis is a developmental process highly susceptible to circadian desynchrony and characterized by coordinated stage-specific organization of clock signaling, mitochondrial homeostasis, and cellular bioenergetics. Chronic circadian desynchrony altered this developmental program, resulting in endocrine instability, altered mitochondrial homeostasis, impaired sperm functional competence, and reduced reproductive success. Collectively, these findings identify disruption of the developmental bioenergetic transition during spermiogenesis as a potential mechanism linking circadian desynchrony with impaired male fertility.

Materials and Methods

Animals and experimental design. All rats were bred and raised in the animal facility of the Department of Biology and Ecology, Faculty of Sciences, University of Novi Sad, Serbia. Adult male Wistar rats (90 days old, P90) were housed under controlled environmental conditions (22 ± 2°C; 14 h light/10 h dark) with food and water available ad libitum. Circadian desynchrony (CD) was induced by repeated weekly cycles consisting of 2 days of constant light, 2 days of constant darkness, and 3 days under a 14 h light/10 h dark photoperiod. Control animals (LD) remained under standard 14 h light/10 h dark conditions. After 2 months, animals were euthanized at ZT11 and ZT23 (n = 5–6 per time point), and testes, epididymides, and serum were collected for subsequent analyses. To analyze the voluntary

activity of the rats, the rats (n = 4) from both light regime groups were placed in individual cages with a running wheel system. The system automatically recorded the total number of wheel turns performed by each animal at 6-minute intervals. The activity pattern was monitored from P90 to P150 (21, 22). To assess reproductive outcome, CD males (n = 20) were individually housed with age-matched control females (n = 20; one pair per cage) for 7 days. Only females exhibiting regular estrous cycles were included. The number of offspring per litter was recorded after parturition. At the end of the experimental period, rats were rapidly euthanized by guillotine decapitation to minimize acute stress-related changes in circulating hormone levels, and testes, epididymides, and blood were immediately collected for subsequent analyses. All procedures were approved by the University of Novi Sad Animal Care Committee (statement No. 01-201/3) and complied with ARRIVE guidelines. The overall experimental workflow, as well as a detailed description of methods, is shown in Supplemental Material.

Seminiferous tubule isolation. Seminiferous tubules were isolated from the testicular interstitial compartment as previously described (22). Briefly, testes were decapsulated, the tunica albuginea and major blood vessels were removed, and testicular tissue was incubated in M199 containing collagenase type IA (0.25 mg/mL), BSA (1.5%), and HEPES (20 mM) for 15 min at 34°C in a shaking water bath (140 cycles/min). Enzymatic digestion was stopped by adding cold M199 containing 0.1% BSA, and the tissue suspension was filtered through a No. 100 mesh to separate seminiferous tubules from the interstitial fraction. The retained tubules were washed three times with PBS by centrifugation (500 × g, 7 min, room temperature) and subsequently used for germ-cell isolation.

Isolation of round and elongated spermatids. Round (RS) and elongated spermatids (ES) were enriched from seminiferous tubules using a modified discontinuous BSA density-gradient sedimentation method based on previously described protocols (23, 24). Briefly, isolated seminiferous tubules were washed twice with prewarmed Krebs buffer and digested with trypsin for 15 min at 34°C in a shaking water bath (120 cycles/min). Digestion was stopped by cooling, followed by filtration through a 40-μm cell strainer and washing with cold Krebs buffer by centrifugation (600 × g, 5 min, 4°C). The resulting cell pellet was resuspended in 0.5% BSA/Krebs buffer and filtered again through a 40-μm cell strainer to obtain a single-cell suspension.

Spermatids were separated by gravitational sedimentation through a discontinuous BSA gradient (0.5%, 1%, and 2% BSA in Krebs buffer) for 1.5 h on ice (24). Fractions enriched in ES and RS were collected from the 0.5% and 1% BSA layers, respectively. Enrichment of the cell populations was verified by DAPI fluorescence microscopy based on characteristic nuclear morphology. Cell number and viability were determined by Trypan Blue exclusion using a Neubauer chamber, with viability exceeding 90%. Cells were subsequently processed for ex vivo experiments or collected by centrifugation (600 × g, 10 min, 4°C) and stored at − 70°C until analysis.

Isolation, capacitation, and acrosome reaction of spermatozoa. Spermatozoa were isolated from the cauda epididymis in modified HBSS containing 1% M199, 20 mM HEPES, and 5% BSA (22). Epididymides were punctured with a needle and incubated for 10 min at 37°C to allow spermatozoa to disperse into

the medium. Spermatozoa were collected by centrifugation (700 × g, 5 min), resuspended in the appropriate medium, and counted using a Makler chamber. For capacitation, approximately 1.5×10^5 spermatozoa were incubated in Whitten's medium supplemented with 10 mg/mL BSA and 20 mM $NaHCO_3$ for 1 h at 37°C. Following capacitation, spermatozoa were incubated with or without progesterone (15 µM) for 30 min at 37°C to induce the acrosome reaction (22). Cells were then fixed, washed, and stained with FITC and DAPI. Acrosome-reacted spermatozoa were quantified by fluorescence microscopy (Zeiss Axio Imager, Carl Zeiss).

Ex vivo treatments. Ex vivo treatments. RS and ES (3×10^6 cells) were seeded in 55-mm Petri dishes containing DMEM/F12 and allowed to attach to the dish surface. Following attachment, 10% fetal bovine serum (FBS; Sigma-Aldrich, St. Louis, MO, USA) was added, and the cells were allowed to recover for 3 h at 34°C in a CO_2 incubator, as previously described (25). Spermatozoa (5×10^6 cells/mL) were resuspended in HBSS and maintained in 1.5-mL tubes. To assess the contribution of oxidative phosphorylation to ATP production, RS, ES, and spermatozoa were treated with oligomycin (20 µM; Sigma-Aldrich) for 2 h. Following treatment, cells and media were collected and stored until analysis.

ATP and mitochondrial function. ATP was quantified using the ATP Bioluminescence CLS II kit (Roche Diagnostics, Mannheim, Germany). Mitochondrial content and mitochondrial membrane potential (ΔΨm) were determined using MitoTracker™ Green FM (Invitrogen, Thermo Fisher Scientific, Waltham, MA, USA) and TMRE (Sigma-Aldrich), respectively, with fluorescence measured on a Fluoroscan Ascent reader (Thermo Labsystems) (21, 22). Protein concentration was determined by the Bradford assay.

Hormone assay. Serum testosterone concentrations were determined by radioimmunoassay using anti-testosterone serum No. 250 supplied by G.D. Niswender (Colorado State University, USA), as previously described (21). All samples were measured in duplicate in one assay (sensitivity: 6 pg/tube; intra-assay coefficient of variation: 5–8%; inter-assay coefficient of variation: 7.5%).

Histomorphometric analysis. Paraffin-embedded testicular sections (4 µm) stained with hematoxylin and eosin were used for histomorphometric analysis. The number of elongated spermatids was determined in stage VII seminiferous tubules (30 tubules per group; n = 3 animals per group). Detailed procedures are described in the Supplemental Methods.

DNA/RNA isolation and gene expression. Genomic DNA was isolated using the NucleoSpin Tissue Kit (Macherey-Nagel, Düren, Germany), whereas total RNA was purified using the GenElute™ Mammalian Total RNA Miniprep Kit (Sigma-Aldrich) or EXTRAsol reagent (BLIRT S.A., Poland). RNA was reverse-transcribed using the High Capacity cDNA Reverse Transcription Kit (Thermo Fisher Scientific). Quantitative PCR was performed with SYBR Green chemistry (Applied Biosystems, Thermo Fisher Scientific) using gene-specific primers (Supplementary Table S1). *Mt-Nd1*/*B2m* ratio was used to estimate mtDNA copy number, and relative mRNA expression was calculated using the 2^−ΔΔCt method with *Gapdh* as the reference gene (21, 22).

Statistics. Depending on the experiment, statistical significance was evaluated using two-way ANOVA, Mann–Whitney, Kruskal–Wallis, Spearman correlation, or principal component analysis (PCA). $P < 0.05$ was considered statistically significant.

Declarations

Ethics approval.

All experimental procedures were conducted in accordance with applicable institutional and national guidelines for the care and use of laboratory animals and were approved by the University of Novi Sad Animal Care Committee (statement No. 01-201/3).

Competing interests.

The authors declare that they have no competing interests.

Declarations of generative AI and AI-assisted technologies in the writing process. During the preparation of this work, the authors used ChatGPT to improve the English language and writing style. After using this tool, the authors reviewed and edited the content as needed and took full responsibility for the content of the manuscript.

Funding.

This study is supported by the Ministry of Science, Technological Development and Innovation of the Republic of Serbia (Grants No. 451-03-137/2025-03/200125).

Author Contribution

TK conceived and designed the study. AB and DL performed the experiments. TK, AB, DL, and SA analyzed and interpreted the data. AB and TK performed statistical analyses and data visualization. TK drafted the manuscript. AB, DL, and SA critically revised the manuscript. All authors read and approved the final manuscript.

Acknowledgement

The authors are very grateful to Vesna Bajagic for technical assistance in experimental performance. The graphic abstract was created with BioRender.com (Publication License no. FY29LFTYG5).

Data Availability

The datasets generated and/or analyzed during the current study are available from the corresponding author on reasonable request.

References

1. Agarwal, A. et al. Male infertility. *Lancet* **397**, 319–333. 10.1016/S0140-6736(20)32667-2 (2021).
2. Sciarra, F. et al. Disruption of circadian rhythms: a crucial factor in the etiology of infertility. *Int. J. Mol. Sci.* **21**, 3943. 10.3390/ijms21113943 (2020).
3. El-Helaly, M., Awadalla, N., Mansour, M. & El-Biomy, Y. Workplace exposures and male infertility: a case-control study. *Int. J. Occup. Med. Environ. Health*. **23**, 331–338. 10.2478/v10001-010-0039-y (2010).
4. Liu, K. et al. Adverse effects of circadian desynchrony on the male reproductive system: an epidemiological and experimental study. *Hum. Reprod.* **35**, 1515–1528. 10.1093/humrep/deaa101 (2020).
5. Gubin, D., Stefani, O., Cornelissen, G. & Touitou, Y. The circadian-light-hygiene hypothesis: a potential modulator of fertility and birthrate trends. *Biology (Basel)*. **15**, 1023. 10.3390/biology15131023 (2026).
6. Kennaway, D. J. The role of circadian rhythmicity in reproduction. *Hum. Reprod. Update*. **11**, 91–101. 10.1093/humupd/dmh054 (2005).
7. Baburski, A. Z. et al. Melatonin replacement restores circadian behavior in adult rat Leydig cells after pinealectomy. *Mol. Cell. Endocrinol.* **413**, 26–35. 10.1016/j.mce.2015.05.039 (2015).
8. Baburski, A. Z. et al. Circadian rhythm of Leydig cell endocrine function is attenuated during aging. *Exp. Gerontol.* **73**, 5–13. 10.1016/j.exger.2015.11.002 (2016).
9. Baburski, A. Z., Andric, S. A. & Kostic, T. S. Luteinizing hormone signaling is involved in synchronization of Leydig cell's clock and is crucial for rhythm robustness of testosterone production. *Biol. Reprod.* **100**, 1406–1415. 10.1093/biolre/ioz020 (2019).
10. Liu, K. et al. Diurnal rhythm of human semen quality: analysis of large-scale human sperm bank data and a timing-controlled laboratory study. *Hum. Reprod.* **37**, 1727–1738. 10.1093/humrep/deac135 (2022).
11. Kimmins, S. & Sassone-Corsi, P. Chromatin remodelling and epigenetic features of germ cells. *Nature* **434**, 583–589. 10.1038/nature03368 (2005).
12. O'Donnell, L. Mechanisms of spermiogenesis and spermiation and how they are disturbed. *Spermatogenesis* **4**, e979623. 10.4161/21565562.2014.979623 (2015).
13. Steger, K. et al. Round spermatids from infertile men exhibit decreased protamine-1 and – 2 mRNA. *Hum. Reprod.* **16**, 709–716. 10.1093/humrep/16.4.709 (2001).
14. de Goede, P., Wefers, J., Brombacher, E. C., Schrauwen, P. & Kalsbeek, A. Circadian rhythms in mitochondrial respiration. *J. Mol. Endocrinol.* **60**, R115–R130. 10.1530/JME-17-0196 (2018).

15. Manella, G. & Asher, G. The circadian nature of mitochondrial biology. *Front. Endocrinol. (Lausanne)*. **7**, 162. 10.3389/fendo.2016.00162 (2016).
16. Kim, J. & Sun, W. Circadian coordination: understanding interplay between circadian clock and mitochondria. *Anim. Cells Syst. (Seoul)*. **28**, 228–236. 10.1080/19768354.2024.2347503 (2024).
17. Park, Y. J. & Pang, M. G. Mitochondrial functionality in male fertility: from spermatogenesis to fertilization. *Antioxid. (Basel)*. **10**, 98. 10.3390/antiox10010098 (2021).
18. Liu, T. et al. The circadian clock orchestrates spermatogonial differentiation and fertilization by regulating retinoic acid signaling in vertebrates. *Natl. Sci. Rev.* **12**, nwae456. 10.1093/nsr/nwae456 (2025).
19. Morse, D., Cermakian, N., Brancorsini, S., Parvinen, M. & Sassone-Corsi, P. No circadian rhythms in testis: period 1 expression is clock independent and developmentally regulated in the mouse. *Mol. Endocrinol.* **17**, 141–151 (2003).
20. Konakchieva, R. et al. Circadian clock deregulation and metabolic reprogramming: a systems biology approach to tissue-specific redox signaling and disease development. *Int. J. Mol. Sci.* **26**, 6267. 10.3390/ijms26136267 (2025).
21. Pavlovic, M. V., Marinkovic, D. Z., Andric, S. A. & Kostic, T. S. The cost of circadian desynchrony on Leydig cell function. *Sci. Rep.* **12**, 15520. 10.1038/s41598-022-19889-9 (2022).
22. Travicic, D. Z. et al. Circadian desynchrony disturbs the function of rat spermatozoa. *Eur. J. Cell. Biol.* **102**, 151323. 10.1016/j.ejcb.2023.151323 (2023).
23. Bryant, J. M., Meyer-Ficca, M. L., Dang, V. M., Berger, S. L. & Meyer, R. G. Separation of spermatogenic cell types using STA-PUT velocity sedimentation. *J. Vis. Exp.* (80), e50648. 10.3791/50648 (2013).
24. Da Ros, M., Heckmann, S. A. & Kotaja, N. Enrichment of pachytene spermatocytes and spermatids from mouse testes using standard laboratory equipment. *J. Vis. Exp.* (151), e60271. 10.3791/60271 (2019).
25. Kavarthapu, R. & Dufau, M. L. Germ cell nuclear factor (GCNF/RTR) regulates transcription of gonadotropin-regulated testicular RNA helicase (GRTH/DDX25) in testicular germ cells: the androgen connection. *Mol. Endocrinol.* **29**, 1792–1804. 10.1210/me.2015-1198 (2015).
26. O'Donnell, L., McLachlan, R. I., Wreford, N. G. & Robertson, D. M. Testosterone promotes the conversion of round spermatids between stages VII and VIII of the rat spermatogenic cycle. *Endocrinology* **135**, 2608–2614 (1994).
27. Zhao, M. et al. Transition nuclear proteins are required for normal chromatin condensation and functional sperm development. *Genesis* **38**, 200–213. 10.1002/gene.20019 (2004).
28. Alvarez, J. D., Chen, D., Storer, E. & Sehgal, A. Non-cyclic and developmental stage-specific expression of circadian clock proteins during murine spermatogenesis. *Biol. Reprod.* **69**, 81–91. 10.1095/biolreprod.102.011833 (2003).
29. Smith, L. B. & Walker, W. H. The regulation of spermatogenesis by androgens. *Semin Cell. Dev. Biol.* **30**, 2–13. 10.1016/j.semcdb.2014.02.012 (2014).

30. Khattri, A. et al. The TNP1 haplotype GCG is associated with azoospermia. *Int. J. Androl.* **34**, 173–182. 10.1111/j.1365-2605.2010.01072.x (2011).
31. Kleene, K. C. & Bagarova, J. Comparative genomics reveals gene-specific and shared regulatory sequences in the spermatid-expressed mammalian Odf1, Prm1, Prm2, Tnp1, and Tnp2 genes. *Genomics* **92**, 101–106. 10.1016/j.ygeno.2008.05.001 (2008).
32. de la Iglesia, A., Jodar, M., Oliva, R. & Castillo, J. Insights into sperm chromatin and implications for male infertility from a protein perspective. *WIREs Mech. Dis.* **15**, e1588. 10.1002/wsbm.1588 (2023).
33. Zalata, A. A., Mokhtar, N., Atwa, A., Khaled, M. & Shaker, O. G. The role of protamine 2 gene expression and caspase 9 activity in male infertility. *J. Urol.* **195**, 796–800. 10.1016/j.juro.2015.08.101 (2016).
34. Pronsato, L., Milanesi, L. & Vasconsuelo, A. Testosterone induces up-regulation of mitochondrial gene expression in murine C2C12 skeletal muscle cells accompanied by an increase of nuclear respiratory factor-1 and its downstream effectors. *Mol. Cell. Endocrinol.* **500**, 110631. 10.1016/j.mce.2019.110631 (2020).
35. Fusco, F. et al. Impact of circadian desynchrony on spermatogenesis: a mini review. *Front. Endocrinol. (Lausanne)*. **12**, 800693. 10.3389/fendo.2021.800693 (2021).
36. Bajpai, M., Gupta, G. & Setty, B. S. Changes in carbohydrate metabolism of testicular germ cells during meiosis in the rat. *Eur. J. Endocrinol.* **138**, 322–327 (1998).
37. Wang, X., Yin, L., Wen, Y. & Yuan, S. Mitochondrial regulation during male germ cell development. *Cell. Mol. Life Sci.* **79**, 91. 10.1007/s00018-022-04134-3 (2022).
38. Amador, A. et al. Distinct roles for REV-ERBα and REV-ERBβ in oxidative capacity and mitochondrial biogenesis in skeletal muscle. *PLoS One*. **13**, e0196787. 10.1371/journal.pone.0196787 (2018).
39. Woldt, E. et al. Rev-erb-α modulates skeletal muscle oxidative capacity by regulating mitochondrial biogenesis and autophagy. *Nat. Med.* **19**, 1039–1046. 10.1038/nm.3213 (2013).
40. Ye, P. et al. BMAL1 regulates mitochondrial homeostasis in renal ischaemia-reperfusion injury by mediating the SIRT1/PGC-1α axis. *J. Cell. Mol. Med.* **26**, 1994–2009. 10.1111/jcmm.17223 (2022).
41. Schmitt, K. et al. Circadian control of DRP1 activity regulates mitochondrial dynamics and bioenergetics. *Cell. Metab.* **27**, 657–666. 10.1016/j.cmet.2018.01.011 (2018).
42. Xu, L. et al. CLOCK regulates Drp1 mRNA stability and mitochondrial homeostasis by interacting with PUF60. *Cell. Rep.* **39**, 110635. 10.1016/j.celrep.2022.110635 (2022).
43. Ren, X., Chen, X., Wang, Z. & Wang, D. Is transcription in sperm stationary or dynamic? *J. Reprod. Dev.* **63**, 439–443. 10.1262/jrd.2016-093 (2017).
44. Castillo, J., Estanyol, J. M., Ballescà, J. L. & Oliva, R. Human sperm chromatin epigenetic potential: genomics, proteomics, and male infertility. *Asian J. Androl.* **17**, 601–609. 10.4103/1008-682X.153302 (2015).
45. Dadoune, J. P. Spermatozoal RNAs: what about their functions? *Microsc Res. Tech.* **72**, 536–551. 10.1002/jemt.20697 (2009).

46. Skowronek, M. F. et al. Morphometric analysis of the sperm midpiece during capacitation. *Tissue Cell.* **95**, 102866. 10.1016/j.tice.2025.102866 (2025).
47. Giaccagli, M. M. et al. Capacitation-induced mitochondrial activity is required for sperm fertilizing ability in mice by modulating hyperactivation. *Front. Cell. Dev. Biol.* **9**, 767161. 10.3389/fcell.2021.767161 (2021).
48. Balbach, M. et al. Metabolic changes in mouse sperm during capacitation. *Biol. Reprod.* **103**, 791–801. 10.1093/biolre/ioaa114 (2020).
49. Kohn, T. P. & Pastuszak, A. W. Shift work is associated with altered semen parameters in infertile men. *Fertil. Steril.* **108**, e323–e324. 10.1016/j.fertnstert.2017.07.956 (2017).
50. Zhang, P., Li, C., Gao, Y. & Leng, Y. Altered circadian clock gene expression in the sperm of infertile men with asthenozoospermia. *J. Assist. Reprod. Genet.* **39**, 165–172. 10.1007/s10815-021-02375-y (2022).

Figures

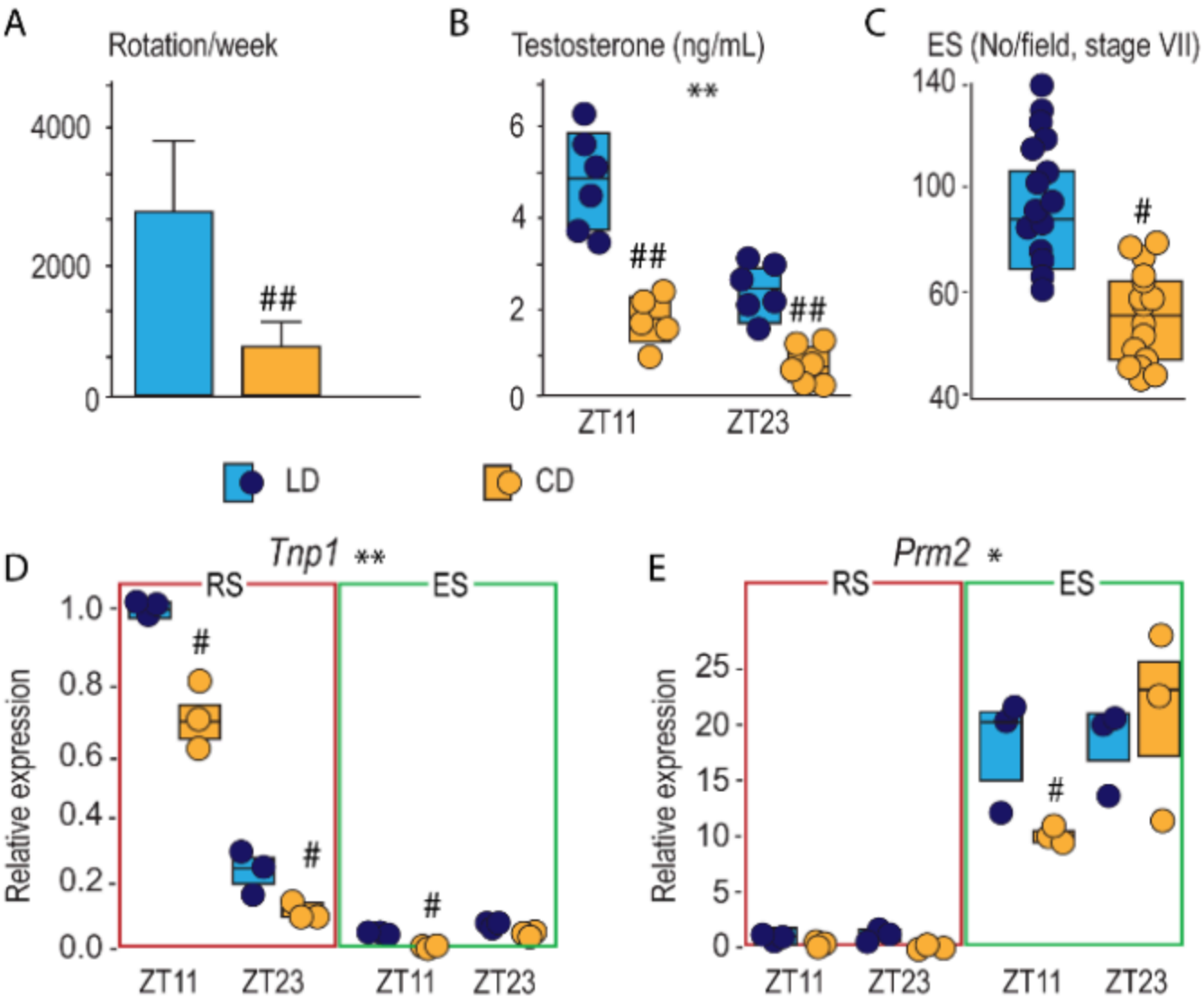


Figure 1

Circadian desynchrony reduces voluntary activity and circulating testosterone and alters spermatid maturation markers. Circadian desynchrony was induced in adult rats by repeated alterations of the light–dark cycle over two months, consisting of 2 days of constant light, 2 days of constant darkness, and 3 days of a 14 h light / 10 h dark schedule, while control animals were maintained under a standard 14:10 light–dark cycle. (A) Representative locomotor activity profiles from the final week of the experiment demonstrate disruption of circadian rhythmicity and reduced voluntary activity in experimental animals compared to controls. (B) Serum testosterone levels measured at ZT11 and ZT23 (ZT0 = lights-on) were significantly reduced in circadian-desynchronized animals, indicating altered endocrine rhythmicity. For gene expression analysis, round spermatids (RS) and elongated spermatids (ES) were isolated from seminiferous tubules. (C) Quantification of ES at stage VII of the seminiferous epithelium, an androgen-dependent and metabolically demanding phase of spermiogenesis. (D-E) Relative expression of the spermatid differentiation markers *Tnp1* and *Prm2* in RS- and ES-enriched fractions. In control animals, *Tnp1*expression was higher in RS compared to ES, with diurnal variation characterized by elevated levels in RS during the inactive phase and the opposite pattern in ES (D). (E) Relative expression of *Prm2*, showing higher abundance in ES compared to RS under control conditions. Circadian desynchrony reduced *Tnp1* transcription in both RS and ES, while *Prm2* expression remained largely unchanged in both cell types. Gene expression data are presented as relative quantification values normalized to RS at ZT11. Values are shown as box-and-whisker plots with individual data points (n = 3–6 per group, two time points). Statistical significance of group differences was assessed using the Kruskal–Wallis test (*$p < 0.05$, ***$p < 0.005$), while differences between corresponding control and experimental groups were evaluated using the Mann–Whitney test (#$p < 0.05$).

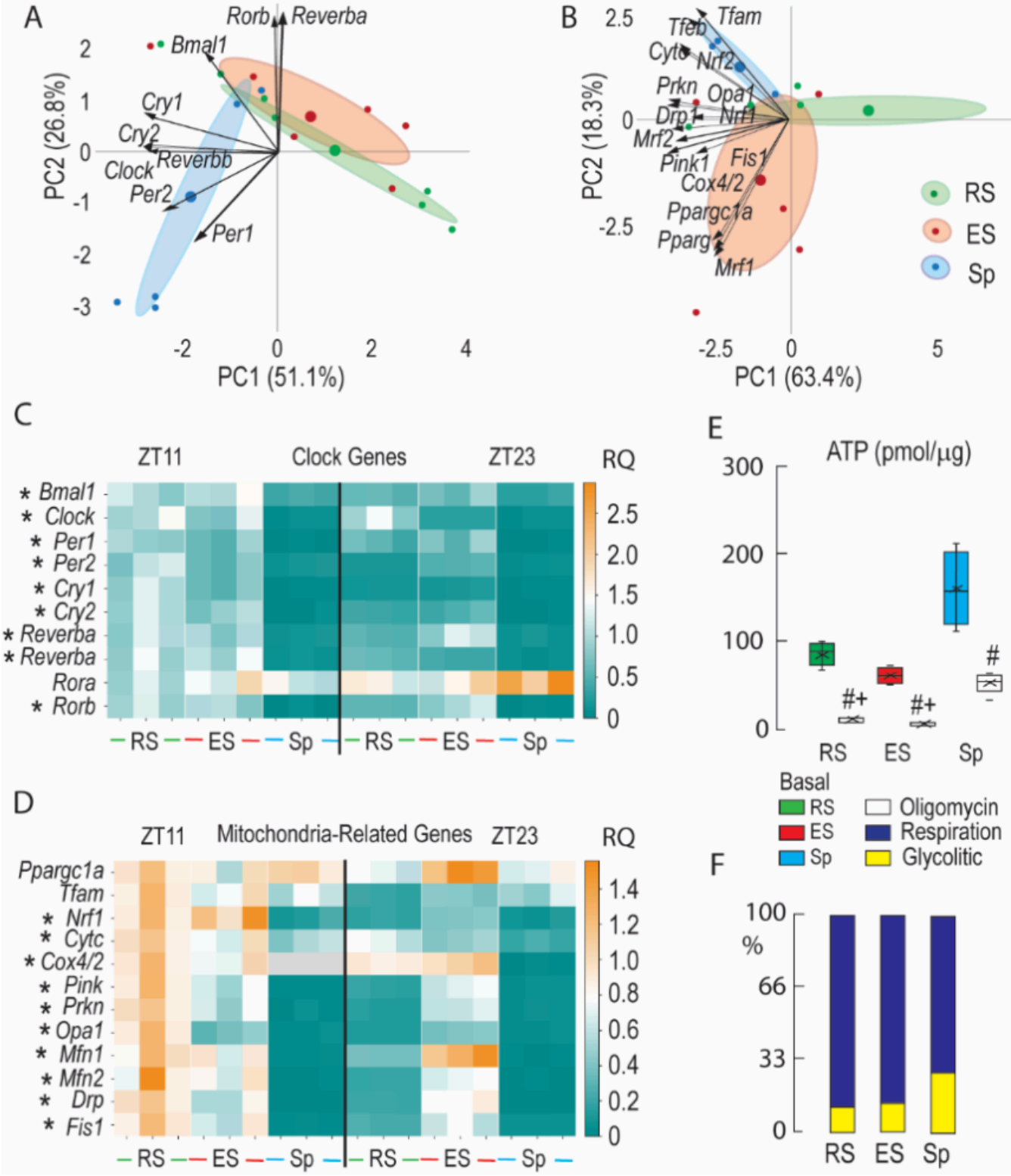


Figure 2

Stage-specific and time-dependent reprogramming of clock and mitochondrial gene expression during spermiogenesis. Testes from control rats were collected at ZT11 and ZT23. Round spermatids (RS) and elongated spermatids (ES) were isolated from seminiferous tubules, while spermatozoa (Sp) were obtained from the epididymis. Relative expression levels of clock genes (A, C) and mitochondria-related genes (B, D) were analyzed in all three cell types. (A–B) Principal component analysis (PCA) score plots

of the first two principal components (PC1 and PC2) derived from clock (A) and mitochondria-related (B) gene expression datasets. Data were normalized to control values at ZT11, which served as the baseline for each cell type. PCA reveals clear stage-dependent separation, with ES occupying an intermediate position between RS and Sp. Mitochondrial gene expression exhibits stronger segregation along the principal components than clock genes, indicating that bioenergetic remodeling is a dominant axis of cellular differentiation. Variable loadings of relative gene expression from PCA are presented in Supplemental Table 2 and 3. (C–D) Heatmap representation of RQ values for (C) clock genes and (D) mitochondria-related genes across individual biological replicates (n = 3), normalized to RS at ZT11. Rows represent genes, and columns correspond to individual samples within each cell type and time point (ZT11 and ZT23). Color intensity reflects relative expression levels from low to high. Clock gene expression (C) shows moderate stage- and time-dependent variation, with an overall reduction in Sp and transitional profiles in ES. In contrast, mitochondria-related genes (D) display a pronounced stage-specific pattern, characterized by higher expression in spermatids and marked suppression in Sp, consistent with progressive bioenergetic reprogramming. (E) RS, ES, and Sp (3×10^6 cells) were incubated in the presence or absence of oligomycin (20 μM) for 2 h at 34°C in 5% CO_2, followed by ATP quantification. (F) Estimated contributions of glycolytic and mitochondrial ATP production. Statistical significance of group differences was assessed using the Kruskal–Wallis test (*p < 0.05). Differences between basal and oligomycin-treated conditions (#p < 0.05), as well as between oligomycin-treated Sp and oligomycin-treated RS/ES (+p < 0.05), were evaluated using the Mann–Whitney test.

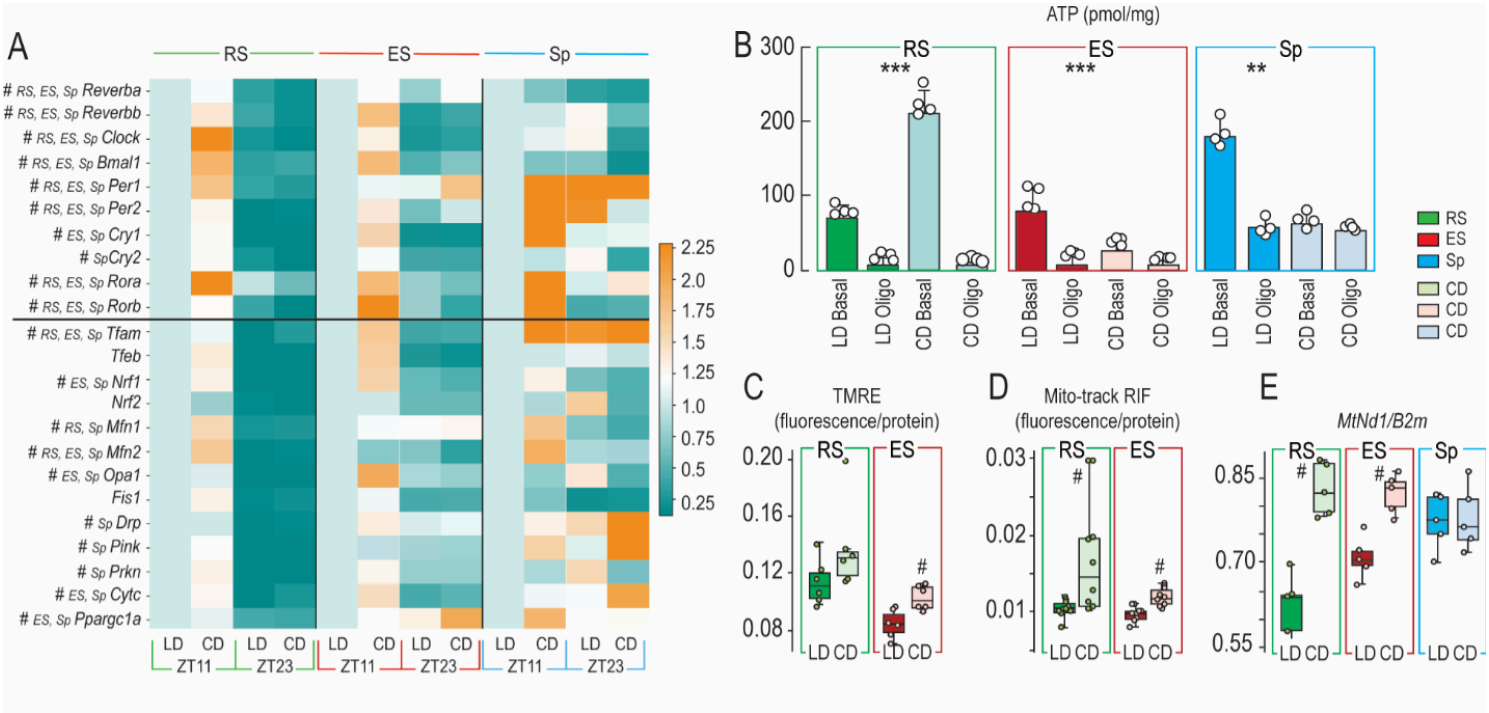


Figure 3

Chronic circadian desynchrony disrupts stage-specific mitochondrial homeostasis during spermiogenesis. Testes from LD and CD rats were collected at ZT11 and ZT23. RS and ES were isolated from seminiferous tubules, while Sp was obtained from the epididymis. (A) The relative expression of

core clock genes and mitochondria-related genes was analyzed in RS, ES, and Sp. The heatmap illustrates gene expression changes under circadian desynchrony across cell types and time points. Data are presented as fold change relative to the corresponding LD controls at ZT11 (n = 3 per group). CD induces widespread alterations in the expression of clock genes and mitochondria-related genes, with more pronounced changes observed during the active phase (ZT23) and in a cell–type–specific manner. (B) ATP content in RS, ES, and Sp under control LD conditions and CD, measured in basal conditions and after oligomycin treatment. Data illustrate the contribution of mitochondrial respiration to ATP production across cell types. (C) Mitochondrial membrane potential (Δψm), assessed by TMRE fluorescence (fluorescence/protein) in RS and ES under LD and CD conditions. (D) MitoTracker Red fluorescence intensity (RIF; fluorescence/protein) in RS and ES, reflecting mitochondrial content under LD and CD conditions. (E) Relative mitochondrial DNA content (*Mt-Nd1*/*B2m* ratio) in RS, ES, and Sp under LD and CD conditions. Data are presented as individual values with mean ± SEM. Statistical significance of group differences was assessed using the Kruskal-Wallis ANOVA test (*p < 0.05, **p < 0.01, ***p < 0.001). The difference between the corresponding LD and CD group (#p < 0.05) was evaluated using the Mann-Whitney test.

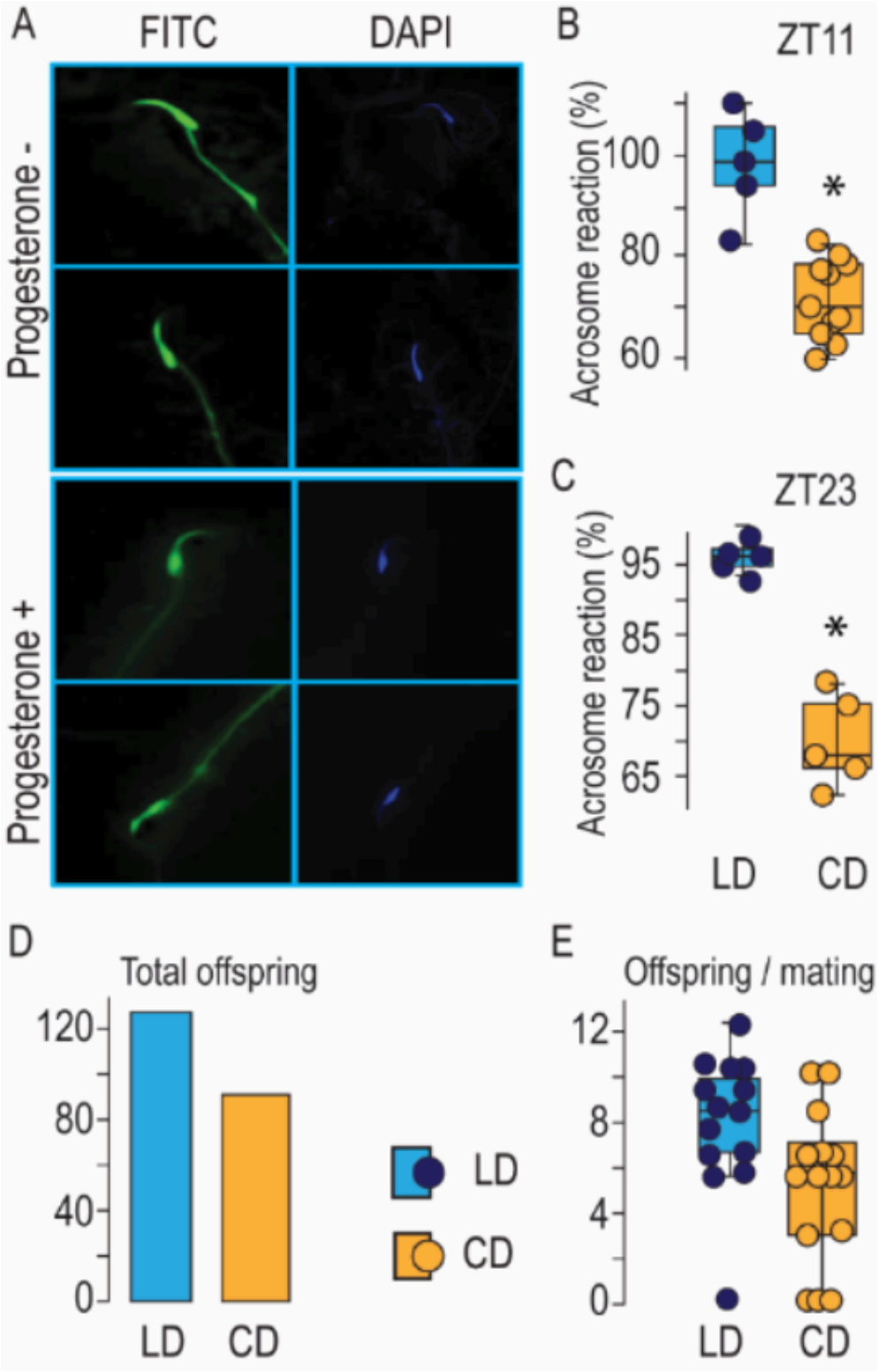


Figure 4

Circadian desynchrony reduces acrosome responsiveness and male reproductive success. Circadian desynchrony impairs spermatozoa function, as assessed by progesterone-induced acrosome reaction. Capacitated spermatozoa were stimulated with progesterone (15 μM). (A) Representative fluorescence images of spermatozoa without (progesterone-) and with progesterone stimulation (progesterone+), showing intact and acrosome-reacted heads of spermatozoa, respectively. Acrosome-reacted

spermatozoa were visualized by FITC staining (green), while nuclei were counterstained with DAPI (blue). (B, C) Quantification of acrosome reaction (% of acrosome-reacted spermatozoa) in LD and CD groups at ZT11 (B) and ZT23 (C) (n = 5–9). (D) Total number of offspring produced by LD and CD males after mating with LD females. (E) Number of offspring per mating in LD and CD groups. Data are presented as individual values with mean ± SEM. Statistical significance was determined using the Mann–Whitney U test (*p < 0.05).

Supplementary Files

This is a list of supplementary files associated with this preprint. Click to download.

- BecinetalSupplementalMatherial.docx